Sub-THz VNA-based Channel Sounder Structure and Channel Measurements at 100 and 300 GHz

Yejian Lyu, Pekka Kyösti, and Wei Fan

***Abstract*—Sub-THz, i.e. frequency range 100 - 300 GHz, frequency bands have attracted huge interest in recent years for beyond 5G communication and high data-rate applications, due to its large available frequency bandwidth. In this work, we presented two vector network analyzer (VNA) based channel sounder systems, operating at the frequency range of 75-110 GHz and 220-330 GHz, respectively. The focus is on the channel sounder structure, link budget as well as system calibration performance. Moreover, we presented a simple wideband directional measurement in a rich scattering laboratory scenario with the two discussed channel sounders. The results showed that similar dominant multipath components (MPCs) can be observed in the two frequency bands, yet many more weak MPCs can be seen at 100 GHz, compared to results at 300 GHz.**

***Index Terms*—Sub-THz, ultra wideband communication, channel sounder, directional channel measurement, channel frequency dependence**

I. Introduction

The ever increasing demands for higher data-rate have motivated the research of sub-terahertz (sub-THz) band, i.e. 100-300 GHz, for the next generation communication systems, due to its large amount of unused spectrum resource. Although sub-THz bands provide an opportunity for high data-rate, many challenges are faced in these bands. Surveys on frequency-dependent free-space path loss and atmospheric attenuation of electromagnetic waves in [1], [2] illustrated that the overall path loss (including free space path loss and atmospheric attenuation) at sub-THz bands becomes very high compared to the lower frequency bands. Moreover, the propagation path can be easily blocked by obstacles. To combat the high attenuation, antennas with high gain and narrow beamwidth are applied [3], [4]. Furthermore, due to the wavelength approaching the size of dust and rain, etc., the behavior of the sub-THz channel might be different compared to the conventional low frequency spectrum [5], [6], which necessitates new channel sounding and modeling studies at those frequency bands.

Until now, a number of channel measurements were performed to investigate the sub-THz channel characteristics. Many efforts on large-scale channel characteristics, i.e., pathloss and shadowing measurements, and delay dispersion analysis and modeling at sub-THz bands in various indoor and outdoor scenarios were made in [7]–[11] at 140 GHz and 300 GHz bands. For the directional channel measurements at sub-THz bands, a double directional indoor channel measurements were conducted at 300 GHz in [12]. Complete channel characteristics such as times of arrival, angles of arrival (AoA) and angles of departure (AoD) in both azimuth and elevation were presented. A measurement-validated frequency domain ray tracing method was also presented and demonstrated to be well-suited to simulate the sub-THz indoor channel. Double directional outdoor measurements across the frequency bands from 141 to 148.5 GHz using vector network analyzer (VNA) based channel sounder with radio-over-fiber (RoF) techniques were conducted in [4]. The results showed large angular spreads of the AoA and AoD. In [13], directional channel measurements at 28 and 140 GHz in a shopping mall scenario were conducted. The delay spread and angular spread of these two bands were found to be similar. After using a cluster-based algorithm to estimate multipath components (MPCs), the results illustrated that the number of MPCs is smaller at 140 GHz than those at 28 GHz. Indoor double directional channel measurements at the millimeterwave and sub-THz bands of 10, 60 GHz and 300 GHz were conducted in [14]. The multipath richness of the radio channel was found to be frequency-dependent, and compared to that of 60 GHz, the multipath richness at 300 GHz decreased. In [15], double directional channel measurements in an intra-wagon scenario were conducted, and the large-scale characteristics, K-factor, delay spread as well as AoAs and AoDs were presented. In addition, measurement-validated ray tracing simulation methods were proposed and utilized to simulate intra-wagon channel model for future beyond 5G system design, deployment, and evaluation.

In this work, we present two vector network analyzer (VNA) based channel sounder systems, operating at the frequency range of 75-110 GHz and 220-330 GHz, respectively. The focus is on the channel sounder structure, link budget as well as system calibration performance. Moreover, we present a wideband directional measurement in a rich scattering laboratory scenario with the two discussed channel sounders. The similarity and difference in the measured channel characteristics between the two sub-THz bands, i.e., 90-110 GHz and 250-300 GHz, are then analyzed.

The rest of this paper is organized as follows. Section II contains two sub-THz channel sounder architecture and performance investigation. Section III describes the directional measurement scenario and highlights the major results at sub-THz bands. Finally, concluding remarks are addressed in Section IV.

Y. Lyu and W. Fan are with the Antennas, Propagation and Millimetre-Wave Systems (APMS) Section, Aalborg University, Aalborg 9220, Denmark.

P. Kyösti is with Oulu University and also with Keysight Technologies Finland Oy.

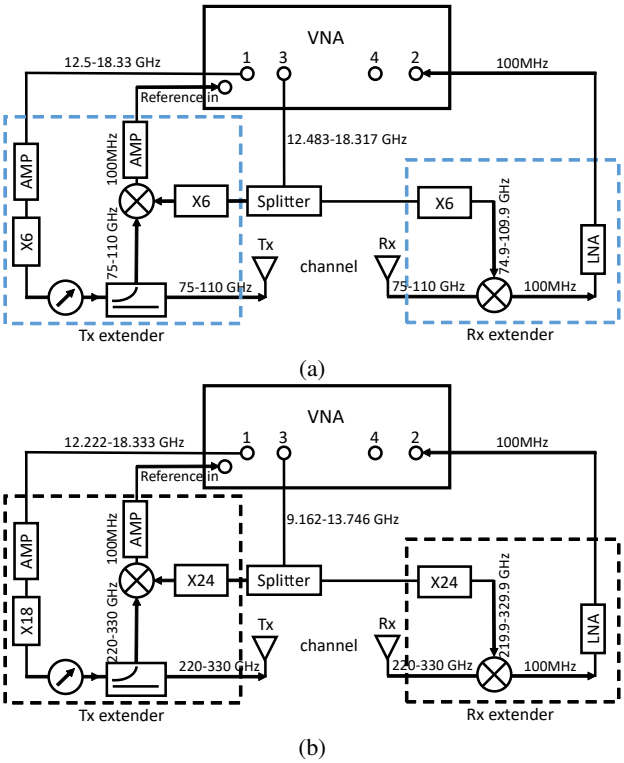

Fig. 1: The schematic diagram the VNA based channel sounder. (a) 75-110 GHz; (b) 220-330 GHz.

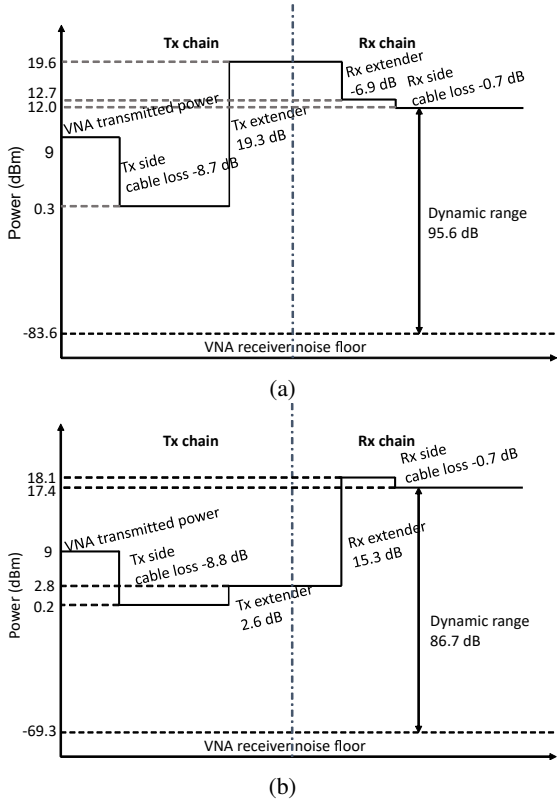

Fig. 2: The link budget of the VNA based channel sounder. (a) 100 GHz channel sounder at 92.5 GHz; (b) 300 GHz channel sounder at 275 GHz.

II. Sounder Architecture and Investigation

A. Sounder architecture

The type of VNA and the frequency extender used in the two sub-THz channel sounders are Keysight N5227B [16], VDI WR 10 [17], and VDI WR3.4 [18], respectively. Fig. 1 illustrate the schematic diagram of the two VNA structure, respectively. For the 100 GHz channel sounder, as shown in Fig. 1 (a), at the transmitter (Tx) side, signals from 12.50 to 18.33 GHz are sent from port 1 resulting in sub-THz signals from 75 to 110 GHz after passing through an 6 times multiplier. The signals are divided into two signals by a coupler, one of which is used to transmit through a horn antenna and the other is used to generate 100 MHz reference signals. Note that port 3 sends local oscillator (LO) signals from 12.48 to 18.32 GHz. The LO signals are split by a signal splitter and multiplied to the frequency range from 74.9 to 109.9 GHz by 6 times multiplier. At the receiver (Rx) side, the received signal is demodulated to 100 MHz, amplified by an LNA and sent to port 2. The S_{21} parameter can be obtained from the result of dividing the 100 MHz received signal by the reference signal. For the channel sounder operating at the frequency range of 220-330 GHz, the sounding structure is similar with the sounder at the frequency range of 75-110 GHz. The main difference is that the multiplier coefficients on the radio frequency (RF) side and LO side are 18 and 24, respectively.

B. Link budget analysis

At the Tx and the Rx side, 5-meter RF cables were used to connect the VNA with the extenders, and the antennas are not included in this link budget analysis. Fig. 2 illustrates the link budget of the channel sounders at 92.5 and 275 GHz. Note that these link budget analysis is only for the measurement settings in this part. The transmitted power from port 1 for both of the channel sounders is 9 dBm to ensure that the Tx extender works normally and to avoid damage. The dynamic range of the 100 GHz channel sounder is 95.6 dB, which is 8.9 dB higher than that of the 300 GHz channel sounder. Compared to high RF cable loss at the Tx side, thanks to the 100 MHz received signal, the RF cable loss is extremely low at Rx side. This two channel sounders can support for the channel measurements at distances below 10 meters (cable limitation). The measurement range can be increased by extending the RF cable length at the Rx side.

C. Calibration investigation

Calibration is essential for channel measurements. Before the channel measurement, a normalization procedure is usually carried out to de-embed the system response in the back-to-back measurement. The objective of our measurement is to verify the efficiency of absorbers placed around the antennas. Firstly, a back-to-back measurement (i.e. without antennas)

TABLE I: The configuration of calibration investigation and directional channel measurements.

Parameter	Value	Value
	100GHz system	300 GHz system
VNA Transmitted power (dBm)	9	
Antenna type	Horn	
Antenna gain (dBi)	21	25
Half-power beamwidth (deg)	19	8
Calibration investigation		
Start frequency (GHz)	75	220
End frequency (GHz)	110	330
Bandwidth	35	110
Frequency point	10001	10001
Tx-Rx distance (m)	0.4	
Antenna height (m)	0.9	
Directional measurement		
Start frequency (GHz)	90	250
End frequency (GHz)	110	300
Bandwidth	20	50
Frequency point	6001	15001
Tx-Rx distance (m)	2.25	
Antenna height (m)	0.9	
Rx azimuth range (deg)	$[-180, 179]$	
Rx rotating step (deg)	1	

and a normalization procedure were conducted to calibrate the system response. Then the comparison channel measurements with and without absorbers at the distance of 0.4 m were conducted (with antennas), as shown in Fig. 3 and Table I. As demonstrated in Fig. 4(a) of the comparison of the channel impulse responses (CIRs) at 100 GHz, the use of the absorbers can significantly eliminate the spurious peaks. However, some very weak unexpected spurious peaks still appeared in the red area. The calibration result with absorbers of the 300 GHz channel sounder is worse than that of the 100 GHz channel sounder, possibly due to huge bandwidth and the non-ideal absorbers for this band. Those small spurious peaks can be eliminated by choosing appropriate bandwidth in the measurements and calibration progress method in the post-processing.

III. Directional Measurement

A. Measurement scenario

These directional measurements were conducted in a laboratory scenario with rich scatterers, as shown in Fig. 5. The measurements were conducted in two sub-THz frequency bands, i.e., 90 to 110 GHz and 250 to 300 GHz. During the measurements at each frequency band, a directional measurement scheme was employed at the Rx side with two identical horn antennas equipped for both Tx and Rx sides. The Tx antenna was fixed, while the bore-sight of the Rx was set to rotate in azimuth within the range of $[-180, 179]$ degree in step of 1 degree, which results in 360 steps in azimuth. Table I illustrates the configuration in the directional channel measurements.

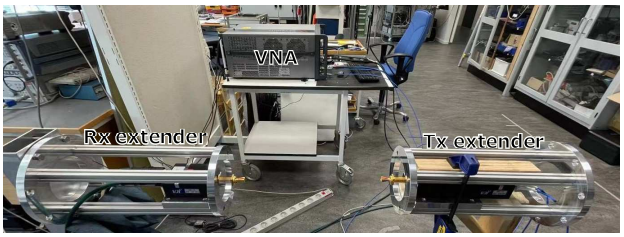

(a)

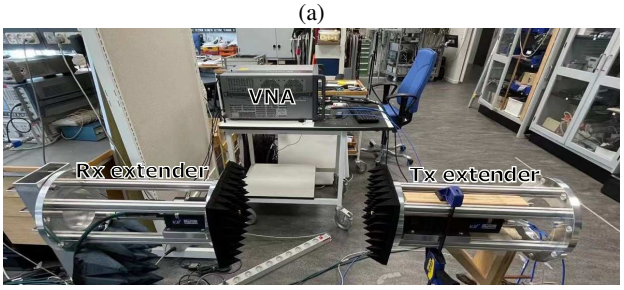

(b)

Fig. 3: The photos of the channel measurement setup. (a) The photo of the channel measurement setup without absorber;(b) The photo of the channel measurement setup with absorber.

B. Signal model

In this study, the channel impulse response (CIR) can be written as:

$$h(t,\tau) = \sum_{\ell=1}^{L} \alpha_\ell \delta\left(\tau - \tau_\ell\right) c(\Omega_\ell), \tag{1}$$

where α_ℓ, τ_ℓ, Ω_ℓ, and L represent the complex attenuation of the ℓth propagation path, the delay of the ℓth propagation path, the direction of arrival (DoA) set of the ℓth MPC, and the total number of propagation paths, respectively.

C. Measurement results

Figure 6 and Figure 7 illustrate the power angular delay profiles (PADPs) from the raw measured data and the relationship between the identified MPCs and the scenario. Note that we only mark the line-of-sight (LoS) path and the main first-order reflection in Figure 6 and Figure 7. The distance of the LoS path (i.e. 2.25 m), which corresponding to 7.5 ns in the measured PADP plots. As shown in Figure 6 and Figure 7, the calculated distances and angles of the main MPCs are found to be well-matched with the scenario. At 100 GHz, the power is concentrated on the LoS direction, and the reflection and scattering of the rich scatterers (e.g. the wall and the screen of the devices) are detected in this scenario. At 275 GHz, the number of MPCs is clearly less than that at 100 GHz, possibly due to the smaller antenna half-power beamwidth (HPBW) and higher path loss. However, compared with 100 GHz, there are similar strong reflections from the platform and the wall at 275 GHz.

IV. Conclusion

In this paper, the system and performance investigations of two channel sounders at sub-THz bands, i.e., 100 GHz and

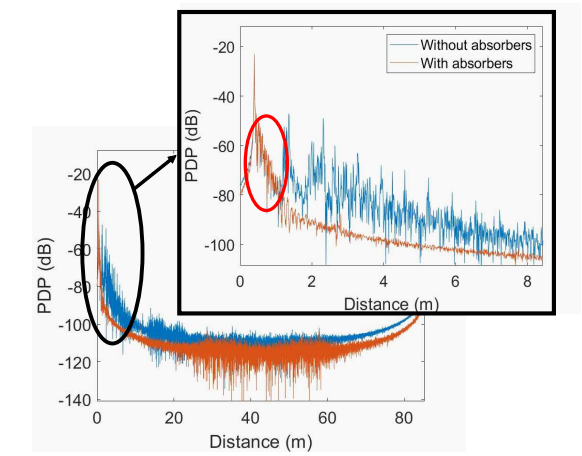

(a)

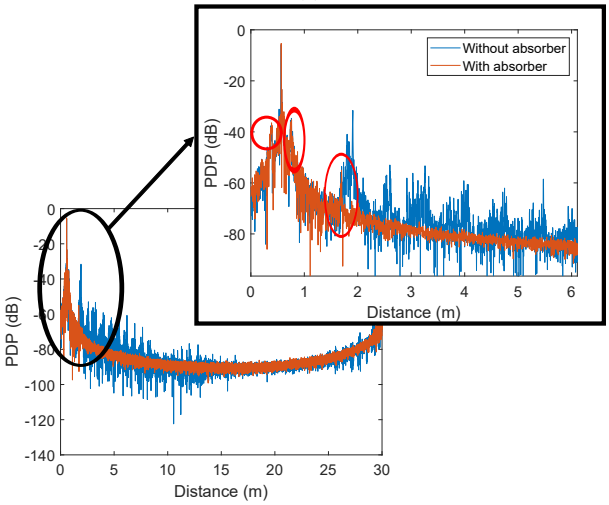

(b)

Fig. 4: The comparison of the CIRs with and without absorbers at the distance of 0.4 m. (a) 100 GHz channel sounder; (b) 300 GHz channel sounder.

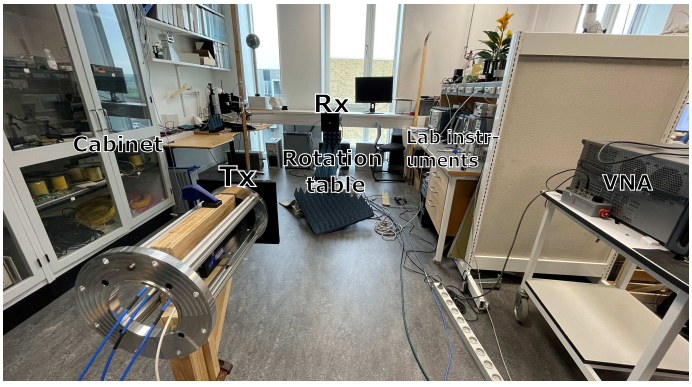

Fig. 5: Picture of the laboratory scenario.

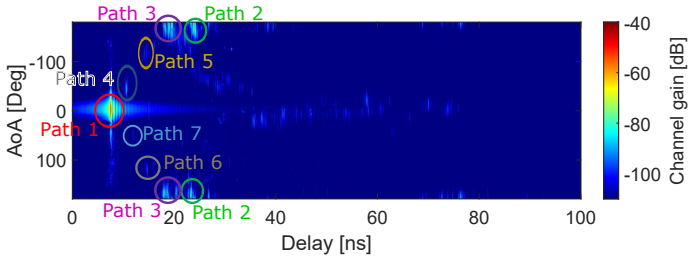

(a)

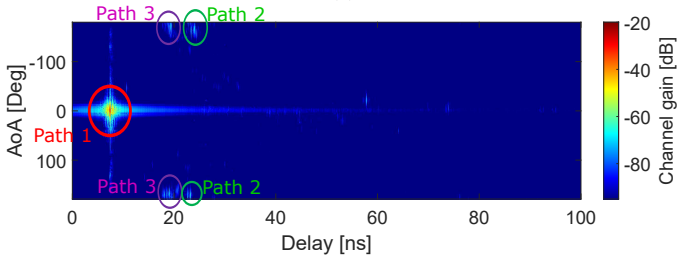

(b)

Fig. 6: PADPs of the directional measurements at (a) 90-110 GHz; (b) 220-330 GHz.

300 GHz, were presented and evaluated. Besides, directional measurements in a laboratory scenario with rich scatterers at those sub-THz bands were conducted, and the results showed that similar dominant MPCs can be observed in these two sub-THz bands, yet many more weak MPCs can be seen at 100 GHz, compared to results at 300 GHz. In our future works, we plan to conduct more in-depth measurements and analysis, including double directional measurements, as well as comparison with ray-tracing simulation.

REFERENCES

[1] J. Ma, R. Shrestha, L. Moeller, and D. M. Mittleman, "Invited article: Channel performance for indoor and outdoor terahertz wireless links," *APL Photonics*, vol. 3, no. 5, p. 051601, 2018. [Online]. Available: https://doi.org/10.1063/1.5014037

[2] A. Pärssinen, M.-S. Alouini, M. Berg, T. Kürner, P. Kyösti, M. E. Leinonen, M. Matinmikko-Blue, E. McCune, U. Pfeiffer, and P. Wambacq, "White paper on RF enabling 6G opportunities and challenges from technology to spectrum," *6G Flagship Ecosystem*, Apr. 2021. [Online]. Available: https://www.6gchannel.com/items/6g-white-paper-rf-spectrum/

[3] T. Kürner and S. Priebe, "Towards THz communications - status in research, standardization and regulation," *Journal of infrared, millimeter and terahertz waves*, vol. 35, no. 1, pp. 53–62, 2014.

[4] N. A. Abbasi, A. Hariharan, A. M. Nair, A. S. Almaiman, F. B. Rottenberg, A. E. Willner, and A. F. Molisch, "Double directional channel measurements for THz communications in an urban environment," in *ICC 2020 - 2020 IEEE International Conference on Communications (ICC)*, 2020, pp. 1–6.

[5] ITU-R, "Attenuation by atmospheric gases," *Recommendation P.676-10*, 2013.

[6] T. S. Rappaport, Y. Xing, O. Kanhere, S. Ju, A. Madanayake, S. Mandal, A. Alkhateeb, and G. C. Trichopoulos, "Wireless communications and applications above 100 GHz: Opportunities and challenges for 6G and beyond," *IEEE Access*, vol. 7, pp. 78 729–78 757, 2019.

[7] S. Priebe, C. Jastrow, M. Jacob, T. Kleine-Ostmann, T. Schrader, and T. Krner, "Channel and propagation measurements at 300 GHz," *IEEE Transactions on Antennas and Propagation*, vol. 59, no. 5, pp. 1688–1698, May 2011.

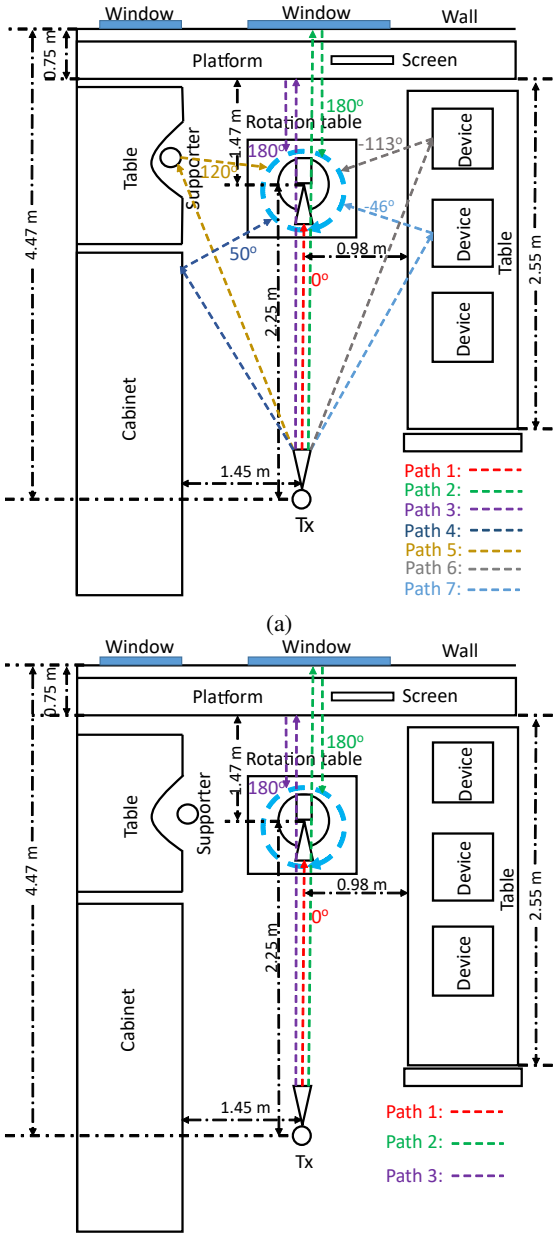

Fig. 7: Relation of the main MPCs to the scenario. (a) 90-110 GHz; (b) 220-330 GHz.

[8] N. Khalid and O. B. Akan, "Wideband THz communication channel measurements for 5G indoor wireless networks," in *2016 IEEE International Conference on Communications (ICC)*, 2016, pp. 1–6.

[9] L. Pometcu and R. DErrico, "An indoor channel model for high data-rate communications in D-band," *IEEE Access*, vol. 8, pp. 9420–9433, 2020.

[10] N. A. Abbasi, A. Hariharan, A. M. Nair, and A. F. Molisch, "Channel measurements and path loss modeling for indoor THz communication," in *2020 14th European Conference on Antennas and Propagation (EuCAP)*, 2020, pp. 1–5.

[11] Y. Xing and T. S. Rappaport, "Propagation measurement system and approach at 140 GHz-moving to 6G and above 100 GHz," in *2018 IEEE Global Communications Conference (GLOBECOM)*, 2018, pp. 1–6.

[12] S. Priebe and T. Kurner, "Stochastic modeling of thz indoor radio channels," *IEEE Transactions on Wireless Communications*, vol. 12, no. 9, pp. 4445–4455, 2013.

[13] S. L. H. Nguyen, J. Jrvelinen, A. Karttunen, K. Haneda, and J. Putkonen, "Comparing radio propagation channels between 28 and 140 GHz bands in a shopping mall," in *12th European Conference on Antennas and Propagation (EuCAP 2018)*, 2018, pp. 1–5.

[14] E. M. Vitucci, M. Zoli, F. Fuschini, M. Barbiroli, V. Degli-Esposti, K. Guan, B. Peng, and T. Kuerner, "Tri-band mm-wave directional channel measurements in indoor environment," in *2018 IEEE 29th Annual International Symposium on Personal, Indoor and Mobile Radio Communications (PIMRC)*, 2018, pp. 205–209.

[15] K. Guan, B. Peng, D. He, J. M. Eckhardt, S. Rey, B. Ai, Z. Zhong, and T. Krner, "Channel characterization for intra-wagon communication at 60 and 300 ghz bands," *IEEE Transactions on Vehicular Technology*, vol. 68, no. 6, pp. 5193–5207, 2019.

[16] K. N5227B. [Online]. Available: https://www.keysight.com/en/pdx-2812784-pn-N5227B/pna-microwave-network-analyzer-67-ghz?&cc=DK&lc=dan

[17] V. W. 10. [Online]. Available: https://www.vadiodes.com/en/wr10-vnax

[18] V. W. 3.4. [Online]. Available: https://www.vadiodes.com/en/wr3-4vnax